Electronic Supplementary Material (ESI) for Journal of Materials Chemistry A.

Supplementary Information

Atomically Manipulated Proton-Transfer Energizes Water Oxidation on Silicon Carbide Photoanodes

Hao Li,[†] *Huan Shang,*[‡] *Yuchen Shi,*[†] *Rositsa Yakimova,*[†] *Mikael Syväjärvi,*[†] *Lizhi Zhang*[‡] *and Jianwu Sun*[*,†]

[†] Department of Physics, Chemistry and Biology, Linköping University, 581 83 Linköping, Sweden

[‡] Key Laboratory of Pesticide & Chemical Biology of Ministry of Education, Institute of Applied &

Environmental Chemistry, College of Chemistry, Central China Normal University, Wuhan 430079,

P. R. China

1. Chemicals

All chemicals used were purchased from Sigma Aldrich.

2. Supporting figures and text

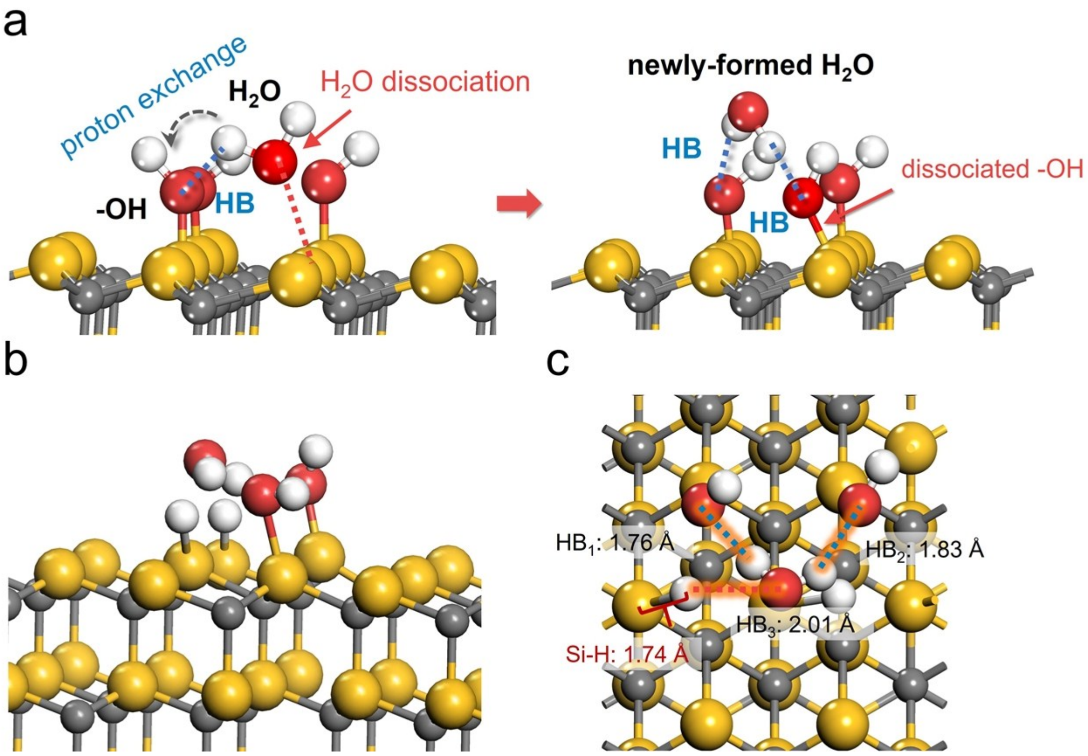

Figure S1. (a) Proton exchange between hydroxyl group of Si-face 6H-SiC and an intimate water molecule. Theoretical modeling of water adsorption on Si face of 6H-SiC(0001) at high coverage: (b) the side view and (c) the top view. Dashed lines show the ordinary HB or hydrogen-like bond.

Figure S1a shows proton exchange between one hydroxyl group (-OH) along with water dissociation towards the formation of a new H_2O molecule, which interacted with hydroxyl groups via strong HBs. The overall reaction can be simply expressed as: $\text{-Si-OH} + H_2O \rightarrow \text{-Si-OH}\ldots H_2O$. When three H_2O were included into a supercell, two of them preferred to dissociate, while the third one chose to form HB network with the two dissociated H_2O (Figure S1b). The HB network contained two strong HBs (HB_1 and HB_2) and one weak HB (HB_3), representing a typical intimate interaction between wetting surface with liquid water (Figure S1c). Besides, the formation of HB_3 lengthened the Si-H bond from 1.50 Å to 1.74 Å.

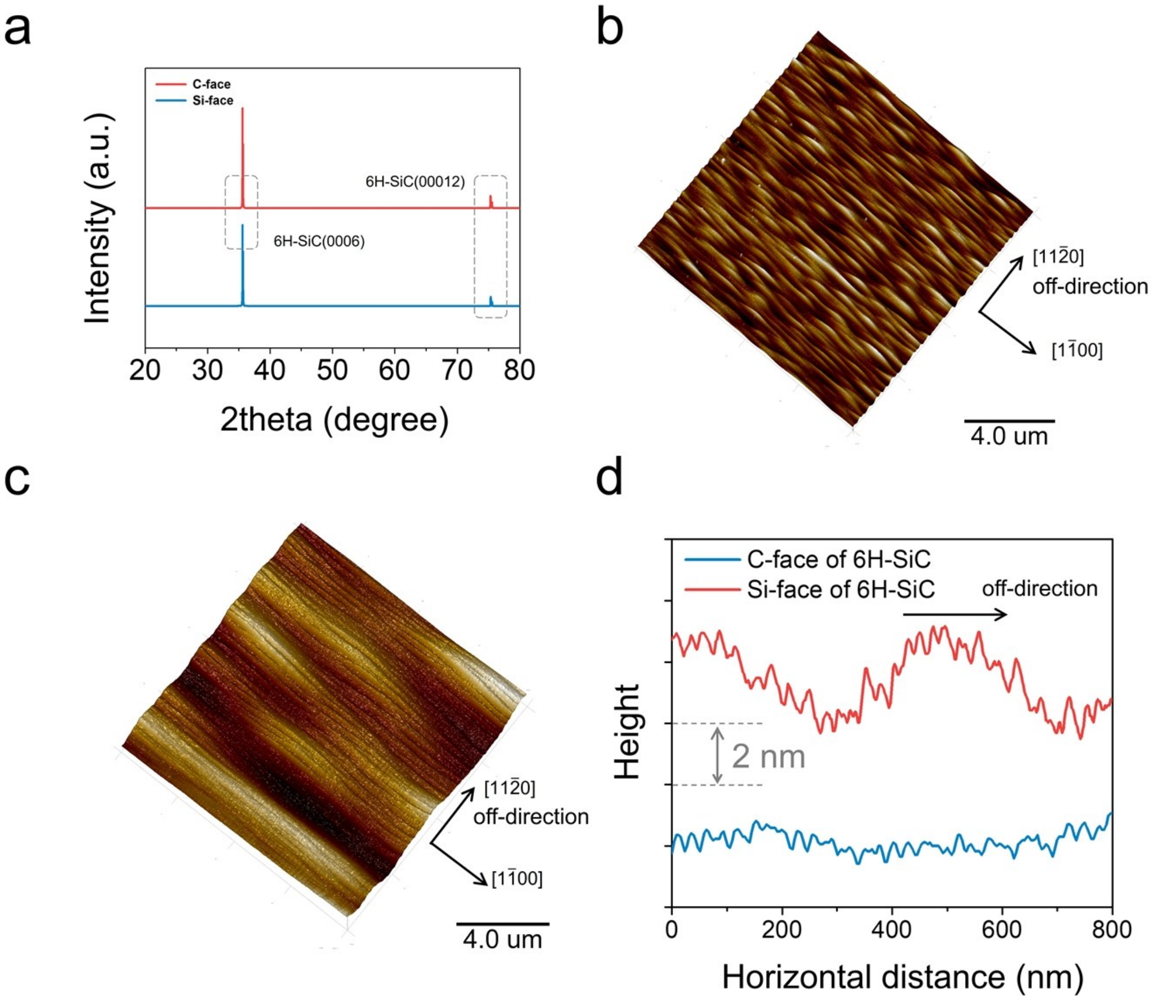

Figure S2. (a) XRD pattern of the as-grown C- and Si- face 6H-SiC films. Atomic force microscopy of the (b) C-face and (c) Si-face of the as-grown 6H-SiC films. (d) Height profiles of the C- and Si-face of the as-grown 6H-SiC films.

Both the as-grown C- and Si-face 6H-SiC films showed two diffracted peaks at 35.5° and 75.5° (Figure S2a). According to the database of joint committee on powder diffraction standards, these two peaks are from 6H-SiC(0006) and 6H-SiC(00012) respectively, suggesting the [0001] growth orientation of the films. Figure S2b shows the atomic force microscopy image of the C-face 6H-SiC, which is composed of "microsteps" during step-flow growth. As for Si-face 6H-SiC, it is different from C-face in that it always contains several "macrosteps" besides the "microsteps" (Figure S2c). Presence of such "macrosteps" is out for a need to minimize the surface energy for the step-flow growth of Si-face SiC epilayer, which is a characteristic feature of Si-face SiC epilayer according to the work reported by Kimoto et al.[1]. Figure S2d shows the height profiles of the 6H-SiC faces and detailed structure of the apparent "macrosteps" can be observed, where many "microsteps" exists.

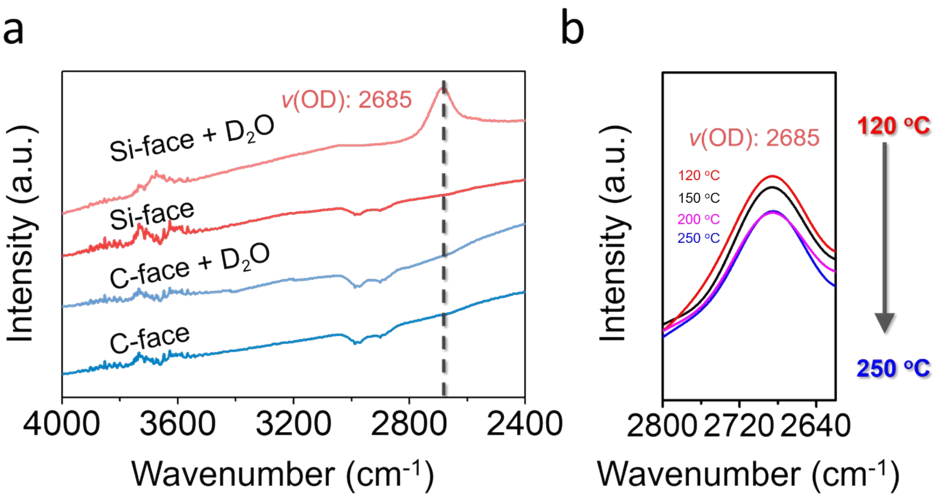

Figure S3. (a) Surface FTIR spectra of the C- and Si-face 6H-SiC before and after heavy water (D_2O) adsorption. (b) Dynamic change of –OD group on Si-face of 6H-SiC along with heating temperature increase.

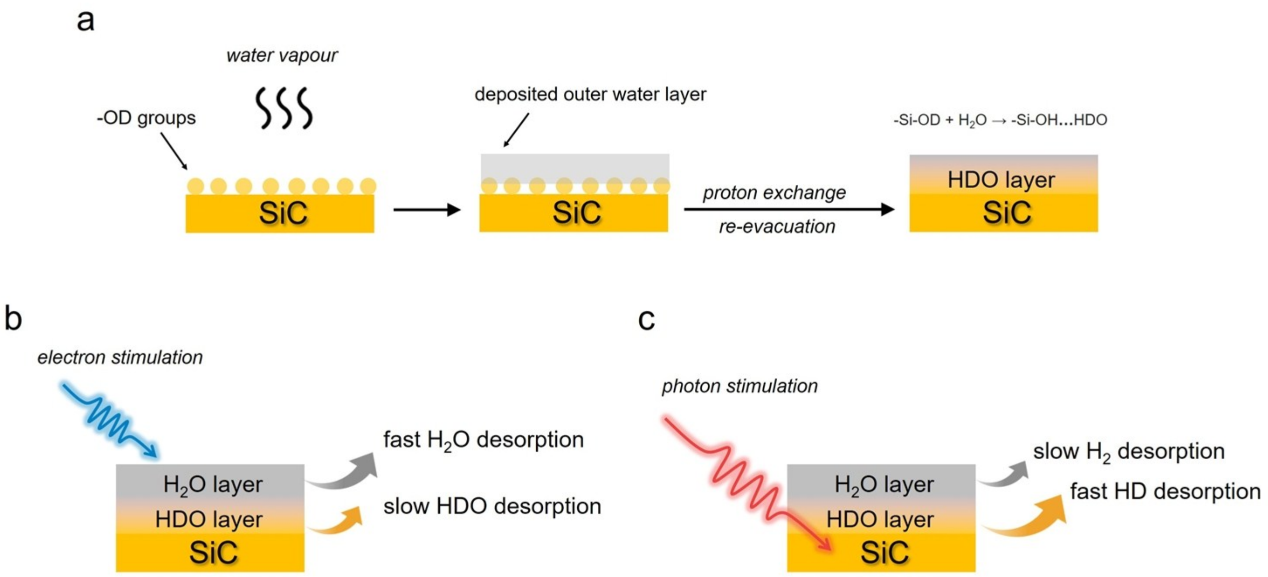

Figure S4. (a) Schematic illustration of the proton exchange process on Si-face of 6H-SiC. (b) Electron-stimulated H_2O desorption. (c) Photon-stimulated H_2 desorption.

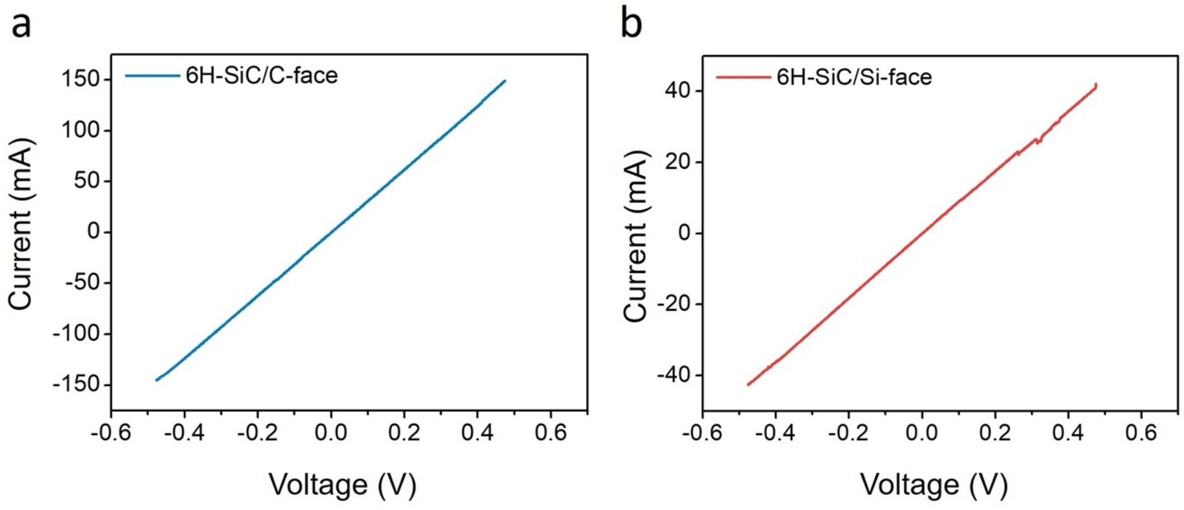

Figure S5. Linear I-V curves of 200-nm Al contacts on backside of the 6H-SiC substrates showing very good Ohmic behavior for both C- and Si-face 6H-SiC photoanodes.

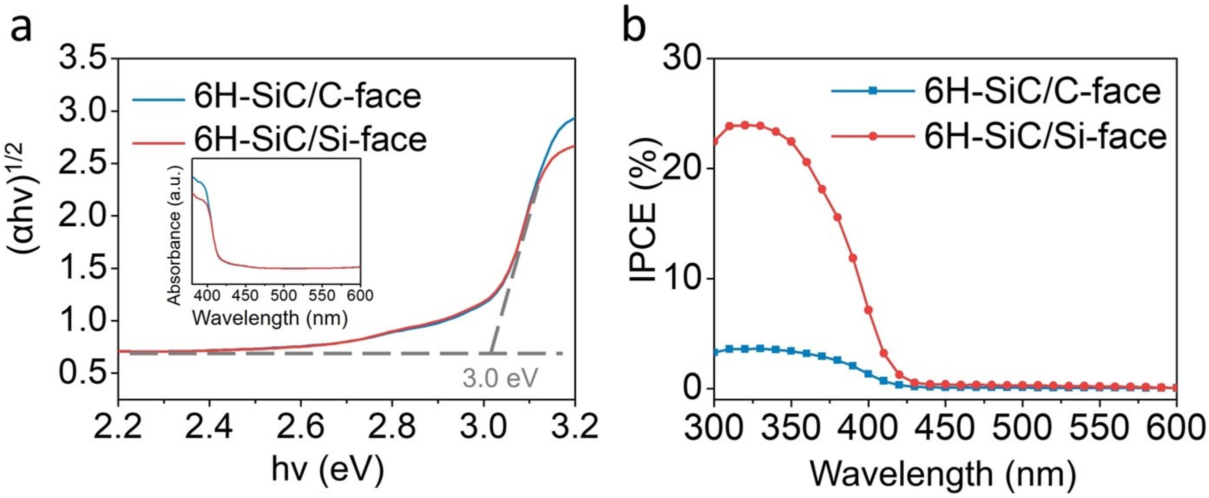

Figure S6. (a) DRS of the as-prepared 6H-SiC films. Data are plotted as transformed Kubelka–Munk function versus the energy of light. Insert shows the absorption spectra. (b) Corresponding incident photon-to-current conversion efficiency under PEC water oxidation condition over the 6H-SiC photoanodes under a moderate bias of 0.4 V_{RHE}.

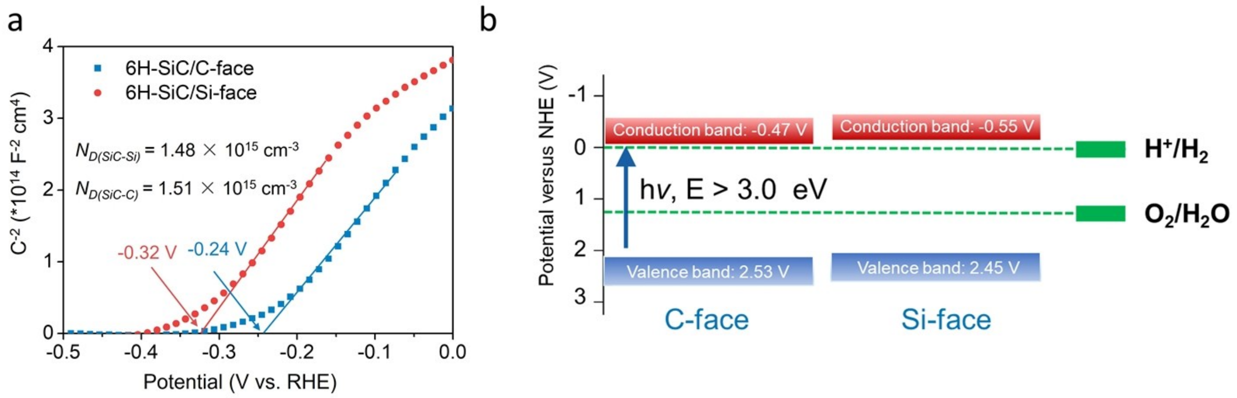

Figure S7. (a) Mott-Schottky plots of the C- and Si- surface 6H-SiC photoanodes and (b) the corresponding band diagram versus water redox potentials.

Figure S7a is the Mott-Schottky plots of the C- and Si- surface 6H-SiC photoanodes that shows the flat band potential to be -0.32 V for the Si-face and -0.24 V for the C-face. According to the almost identical doping concentration, conduction band potential is determined to be -0.55 V for the Si-face and -0.47 V for the C-face. Therefore, valence band potential for Si-face and C-face is considered as comparable with a small difference of 0.08 V.

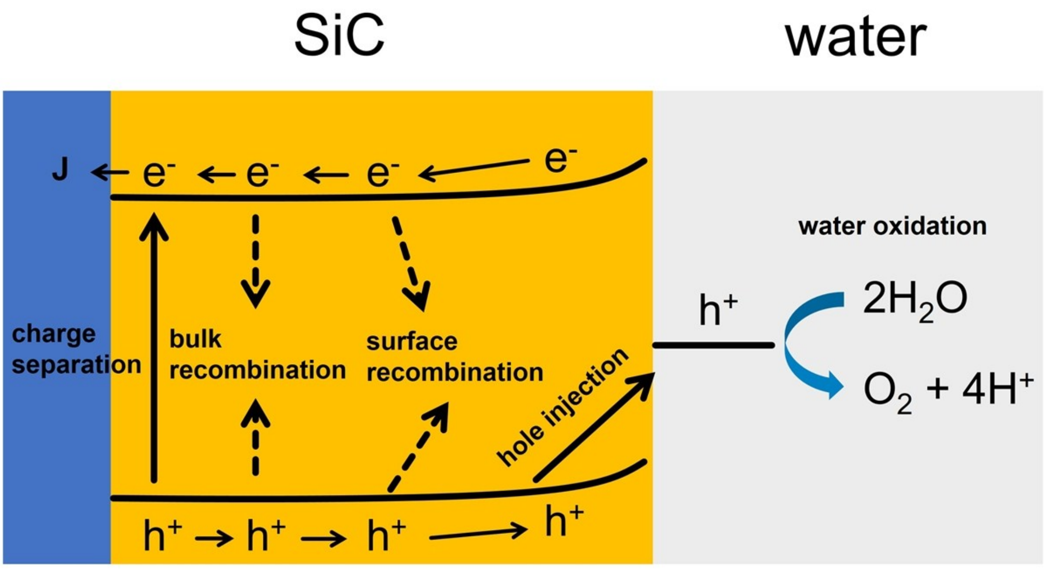

Figure S8. Schematic illustration of the charge transfer processes associated with photoelectrochemical water oxidation on SiC, which included photogenerated carriers via light absorption, bulk recombination, surface recombination, and charge injection to electrolyte for water oxidation.

J_{abs} is the photocurrent density of SiC assuming the absorbed photon conversion efficiency to be 100%. Upon light absorption, part of J_{abs} is lost due to bulk recombination and surface recombination. Therefore, the measured photocurrent density J arising from OER is theoretically described as $J = J_{abs}\phi_{sep}\phi_{ox}$, where ϕ_{sep} represents charge separation yield of the photogenerated carriers in bulk and/or surface, and ϕ_{ox} represents the quantum efficiency of the water oxidation by holes that have reached the surface without annihilation. For an easily oxidized surrogate substrate like H_2O_2, surface recombination is completely suppressed with $\phi_{ox} = 1$. Therefore, when probing water oxidation using the same electrode, ϕ_{ox} can be calculated from the ratio of $J^{H_2O}/J^{H_2O_2}$.

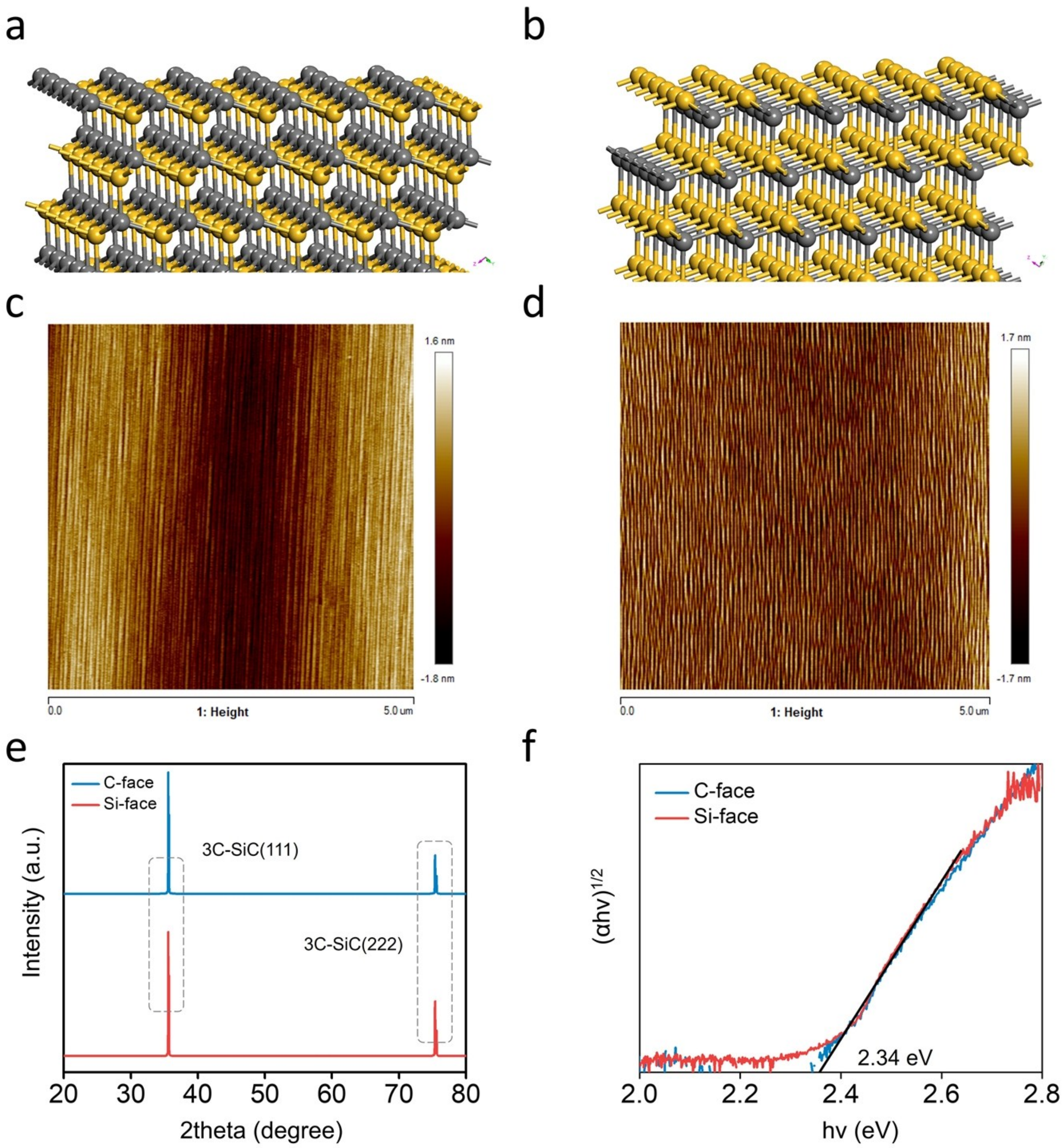

Figure S9. Schematic illustration of surface structure of (a) C-face and (b) Si-face of 3C-SiC(111). Atomic force microscopy of the (c) C-face and (d) Si-face of 3C-SiC(111). (e) XRD pattern of the as-grown 3C-SiC single-crystalline films. (f) DRS of the as-prepared free-standing 3C-SiC single crystalline film. Data are plotted as transformed Kubelka–Munk function versus the energy of light.

Alternating stacking of C- and Si-layer along the [111] axis growth makes the (111) face exposed (Figure S9a and S9b). Atomic force microscopy revealed both C-face and Si-face of 3C-

SiC(111) was composed microsteps of comparable height and width along with the step-flow growth (Figure S9c and S9d). According to the XRD pattern, the 3C-SiC films are clearly epitaxial, with only (111) and (222) peaks appearing at 35.8° and 75.6°, respectively (Figure S9e). No other SiC polytypes or orientations are present. Meanwhile, the as-grown 3C-SiC films have identical bandgap according to their DRS spectra.

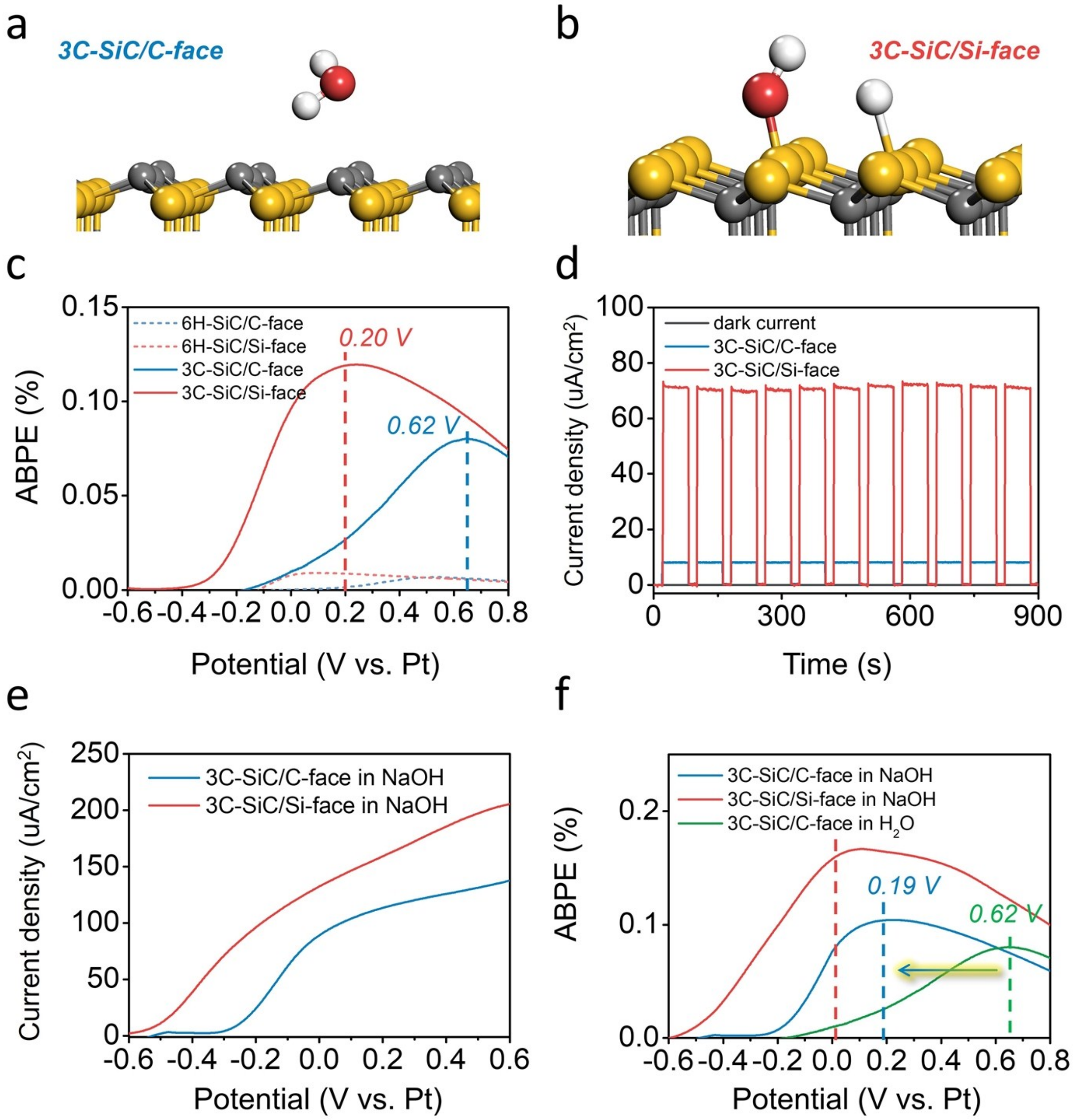

Figure S10. Theoretically modeled water adsorption on the (a) C-face and (b) Si-face of 3C-SiC(111) surface. (c) ABPE of the 3C-SiC and 6H-SiC photoanodes in 0.5 M pH 6.8 Na_2SO_4 in two-electrode system. (d) Unbiased water splitting photocurrent for the C- and Si- face 3C-SiC photoanode short-circuited to Pt in 0.5 M pH 6.8 Na_2SO_4 under chopped illumination in two-electrode system. (e) *J-V* curves measured for 3C-SiC photoanodes with both C- and Si- faces in 1.0 M NaOH in two-electrode system and (f) the corresponding ABPE. Illumination: AM1.5G 100 mW/cm^2.

Reference:

(1) Kimoto, T.; Itoh, A.; Matsunami, H. *Appl. Phys. Lett.* **1995**, *66* (26), 3645.